LEPTON PHOTON 2021 MAN

भारतीय प्रौद्योगिकी संस्थान गुवाहाटी
INDIAN INSTITUTE OF TECHNOLOGY GUWAHATI

Within and beyond the SM via b→u decays

Based on JHEP 07 (2021) 082 and JHEP 09 (2021) 127. In collaboration with Soumitra Nandi, Ipsita Ray and Sunando Patra. On behalf of csbiitg.

Prologue

- Exclusive $B \to \pi, \rho\ l\nu$ decays: $|V_{ub}|$ extraction. $l = e, \mu$. Insensititive to NP. $l = \tau$ sensitive to NP.
- **Inclusive measurement:** Considerable background from $b \to c l\nu$ decays. Experimental cuts required to separate $b \to u$ from $b \to c$ decays. Restricts phase space. OPE breaks down and sensitivity to non-perturbative aspects increases.
- **Exclusive measurement:** $B \to \pi l\nu$ decays. HFLAV methodology. Babar(2011) (Phys. Rev. D **83**(2011) 032007), Belle(2011) (Phys. Rev. D **83** (2011) 071101), Babar (2012) (Phys. Rev. D **86** (2012) 092004), Belle(2013) (Phys. Rev. D **88** (2013) 032005). Averaging (p-value$\sim 6\%$) followed by fitting $|V_{ub}|$to averaged dataset. Significance less. Biased result.
- Disagreement of ≥ 2.2 σ. V_{ub}^{incl}:$(3.70 \pm 0.16) \times 10^{-3}$ V_{ub}^{excl}:$(4.25 \pm 0.12^{+0.15}_{-0.14}) \times 10^{-3}$.
- Remember R(D$^{(*)}$) from $b \to c l\nu$ decays. Define NP observables which are ratios of τ: e, μ. Cancel $|V_{ub}|$ which is the dominant source of uncertainty. Errors: Form factors.

The Theory

$$\mathcal{H}_{\text{eff}} = \frac{4G_F}{\sqrt{2}} V_{ub} \left[(1 + C_{V_1}) \mathcal{O}_{V_1} + C_{V_2} \mathcal{O}_{V_2} + C_{S_1} \mathcal{O}_{S_1} + C_{S_2} \mathcal{O}_{S_2} + C_T \mathcal{O}_T \right]$$

$$\begin{aligned}
\mathcal{O}_{V_1} &= (\overline{u}_L \gamma^\mu b_L)(\overline{\tau}_L \gamma_\mu \nu_L)\,, \\
\mathcal{O}_{V_2} &= (\overline{u}_R \gamma^\mu b_R)(\overline{\tau}_L \gamma_\mu \nu_L)\,, \\
\mathcal{O}_{S_1} &= (\overline{u}_L b_R)(\overline{\tau}_R \nu_L)\,, \\
\mathcal{O}_{S_2} &= (\overline{u}_R b_L)(\overline{\tau}_R \nu_L)\,, \\
\mathcal{O}_T &= (\overline{u}_R \sigma^{\mu\nu} b_L)(\overline{\tau}_R \sigma_{\mu\nu} \nu_L)\,.
\end{aligned}$$

$$\begin{aligned}
&\frac{d\Gamma(\overline{B} \to \pi \tau \overline{\nu})}{dq^2} \\
&= \frac{G_F^2 |V_{ub}|^2}{192\pi^3 m_B^3} q^2 \sqrt{\lambda_\pi(q^2)} \left(1 - \frac{m_\tau^2}{q^2}\right)^2 \times \left\{ |1 + C_{V_1} + C_{V_2}|^2 \left[\left(1 + \frac{m_\tau^2}{2q^2}\right) H_{V,0}^{s\,2} + \frac{3}{2} \frac{m_\tau^2}{q^2} H_{V,t}^{s\,2} \right] \right. \\
&\quad + \frac{3}{2} |C_S|^2 H_S^{s\,2} + 8 |C_T|^2 \left(1 + \frac{2m_\tau^2}{q^2}\right) H_T^{s\,2} + 3\mathcal{R}e[(1 + C_{V_1} + C_{V_2})(C_S^*)] \frac{m_\tau}{\sqrt{q^2}} H_S^s H_{V,t}^s \\
&\quad \left. - 12\mathcal{R}e[(1 + C_{V_1} + C_{V_2}) C_T^*] \frac{m_\tau}{\sqrt{q^2}} H_T^s H_{V,0}^s \right\}
\end{aligned} \tag{2.3}$$

$$\begin{aligned}
&\frac{d\Gamma(\overline{B} \to \rho \tau \overline{\nu})}{dq^2} \\
&= \frac{G_F^2 |V_{cb}|^2}{192\pi^3 m_B^3} q^2 \sqrt{\lambda_\rho(q^2)} \left(1 - \frac{m_\tau^2}{q^2}\right)^2 \times \left\{ (|1 + C_{V_1}|^2 + |C_{V_2}|^2) \left[\left(1 + \frac{m_\tau^2}{2q^2}\right) \left(H_{V,+}^2 + H_{V,-}^2 + H_{V,0}^2\right) \right. \right. \\
&\quad \left. + \frac{3}{2} \frac{m_\tau^2}{q^2} H_{V,t}^2 \right] - 2\mathcal{R}e[(1 + C_{V_1}) C_{V_2}^*] \left[\left(1 + \frac{m_\tau^2}{2q^2}\right) \left(H_{V,0}^2 + 2H_{V,+} H_{V,-}\right) + \frac{3}{2} \frac{m_\tau^2}{q^2} H_{V,t}^2 \right] \\
&\quad + \frac{3}{2} |C_P|^2 H_S^2 + 8 |C_T|^2 \left(1 + \frac{2m_\tau^2}{q^2}\right) \left(H_{T,+}^2 + H_{T,-}^2 + H_{T,0}^2\right) + 3\mathcal{R}e[(1 + C_{V_1} - C_{V_2}) \\
&\quad C_P^*] \frac{m_\tau}{\sqrt{q^2}} H_S H_{V,t} - 12\mathcal{R}e[(1 + C_{V_1}) C_T^*] \frac{m_\tau}{\sqrt{q^2}} (H_{T,0} H_{V,0} + H_{T,+} H_{V,+} - H_{T,-} H_{V,-}) \\
&\quad \left. + 12\mathcal{R}e[C_{V_2} C_T^*] \frac{m_\tau}{\sqrt{q^2}} (H_{T,0} H_{V,0} + H_{T,+} H_{V,-} - H_{T,-} H_{V,+}) \right\}
\end{aligned} \tag{2.5}$$

Inputs

- $B \to \pi, \rho\ l\nu$: Babar(2011) (Phys. Rev. D **83**(2011) 032007), Belle(2011) (Phys. Rev. D **83** (2011) 071101), Babar (2012) (Phys. Rev. D **86** (2012) 092004), Belle(2013) (Phys. Rev. D **88** (2013) 032005).

- $B \to \pi$ **Form Factors:** Lattice (high q^2): MILC(*Phys. Rev. D* **92** (2015) 014024, *PoS* **LATTICE 2019** (2019) 236), UKQCD(*Phys. Rev. D* **91** (2015) 074510). **Tensor:** NP analysis. , Lattice: MILC *(Phys. Rev. Lett.* **115** (2015) 152002). LCSR(low q^2): GKD (*JHEP* **01** (2019) 150) , LMD (*JHEP* **07** (2021) 036). LMD use two-particle twist-two pion LCDA. More precise than GKD which is an LO calculation with the ill-known B-meson LCDA.

- $B \to \rho$ **Form Factors**: No Lattice Data. LCSR(low q^2): GKD (*JHEP* **01** (2019) 150). BSZ (*JHEP* **08** (2016) 098). BSZ:twist-3 $O(\alpha_s)$ using the ρ meson LCDA. More precise than GKD, who use narrow width approximation.

- **Form Factors Parametrizations**: BSZ(*JHEP* **08** (2016) 098); BCL(*Phys. Rev. D* **79** (2009) 013008).

$|V_{ub}|$ Extraction: Our Strategy

- DO NOT AVERAGE!. Look for outliers using both inclusive and exclusive $|V_{ub}|$. Common outliers are problematic.
- Plots using $|V_{ub}|$ inclusive $(4.10 \pm 0.22 \pm 0.22 \pm 0.22) \times 10^{-3}$ (Belle).

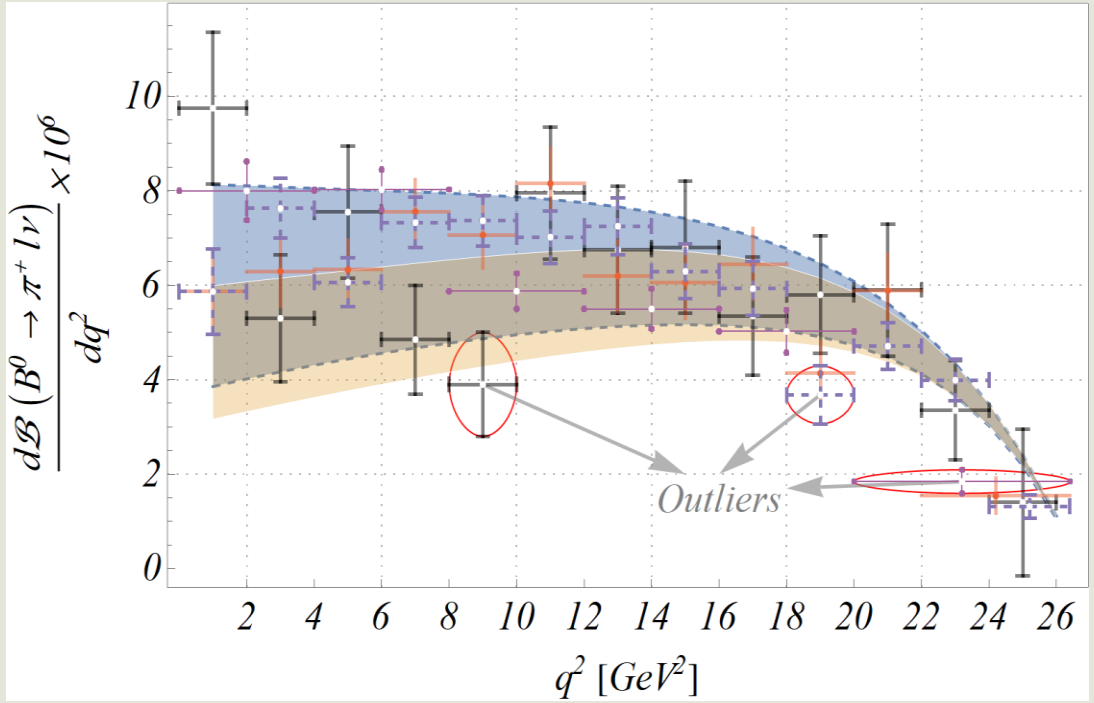

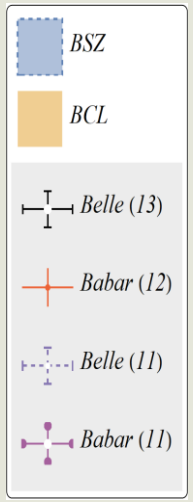

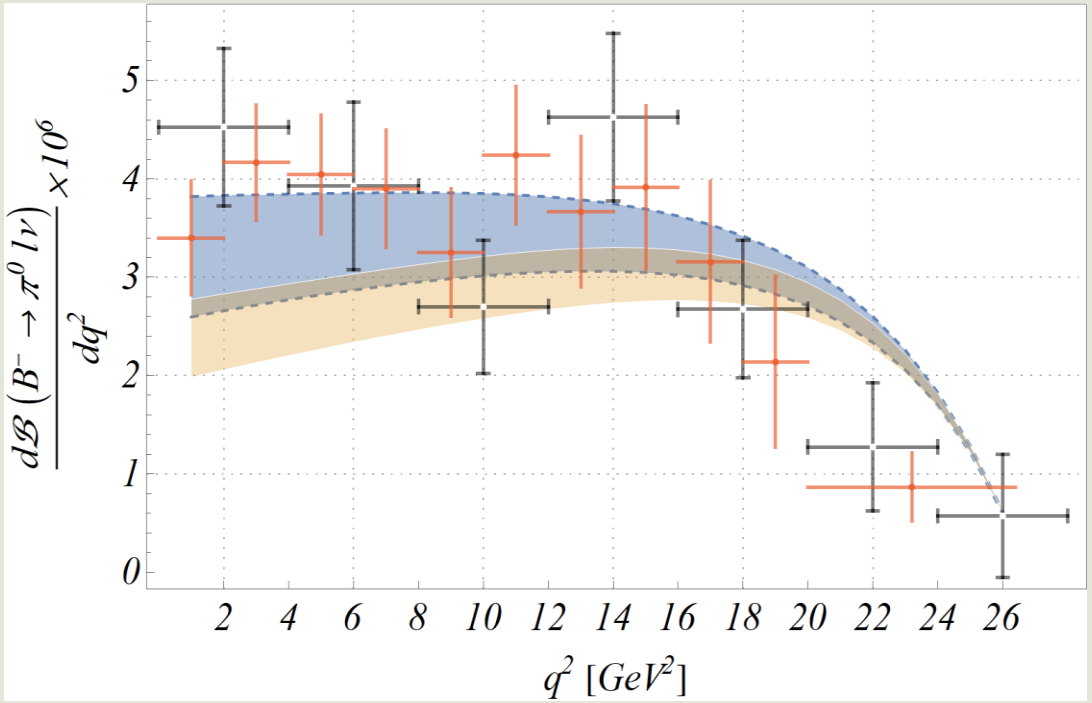

$|V_{ub}|$ Extraction: Analysis

- **Fit 1**: B^0 decays from Belle (2011) and Belle (2013); B^- decays from Belle (2013); the combined modes from BaBar (2011) and BaBar (2012). We have subdivided this set into two sets depending on whether or not LCSR inputs are taken into account, like the following:
  1. *Fit 1A*: experimental data (Fit 1) + synthetic Lattice data points,
  2. *Fit 1B*: experimental data (Fit 1) + synthetic Lattice data points + LCSR.
- **Fit 2**: B^0 decays from Belle (2011), BaBar (2012), and Belle (2013); B^- decays from BaBar (2012) and Belle (2013). As above we have defined the following sets:
  - *Fit 2A*: experimental data (Fit 2) + synthetic Lattice data points,
  - *Fit 2B*: experimental data (Fit 2) + synthetic Lattice data points + LCSR.
- **Fit 3**: the combined modes from BaBar (2011) along with the *Fit 2* dataset, with and without LCSR as follows:
  - *Fit 3A*: experimental data (Fit 3) + synthetic Lattice data points,
  - *Fit 3B*: experimental data (Fit 3) + synthetic Lattice data points + LCSR.

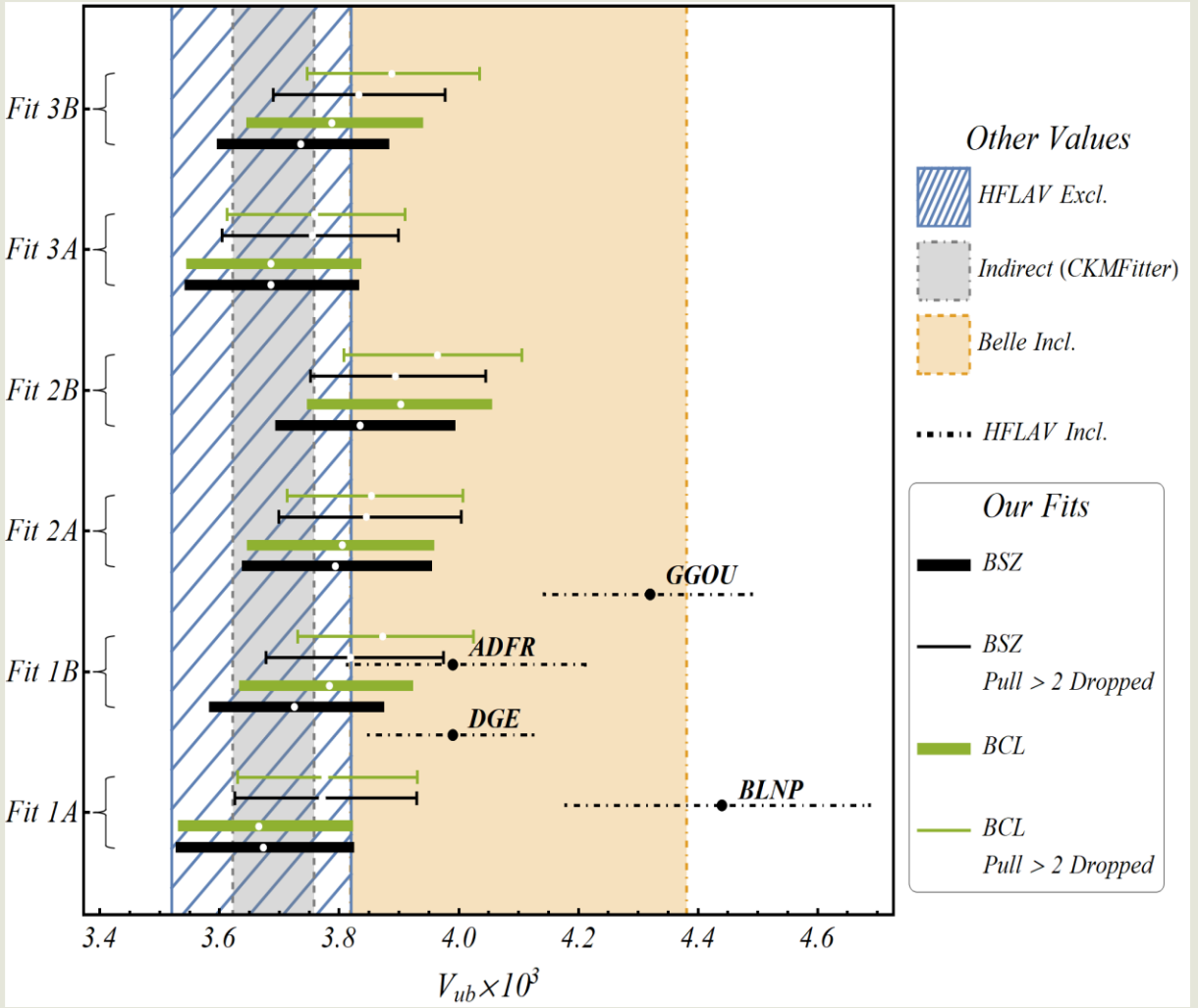

$|V_{ub}|$ Extraction: Results

Form-Factors	Inclusive V_{ub} used	$[B^0 \to \pi^-]$ q^2 : 18 – 20 Belle (11)	$[B^0 \to \pi^-]$ q^2 : 20 – 26.4 BaBar (11)	$[B^0 \to \pi^-]$ q^2 : 18 – 20 BaBar (12)	$[B^+ \to \pi^0]$ q^2 : 20 – 26.4 BaBar (12)	$[B^0 \to \pi^+]$ q^2 : 0.0111637 – 2 Belle (13)	$[B^0 \to \pi^+]$ q^2 : 8 – 10 Belle (13)
BSZ	HFLAV (GGOU)	−2.55	−3.54	−2.13	−2.35	—	−2.04
	HFLAV (BLNP)	−2.50	−3.27	−2.14	−2.41	—	−2.09
	Belle (New)	—	−2.32	—	—	2.22	—
BCL	HFLAV (GGOU)	−2.32	−3.49	—	−2.28	2.30	—
	HFLAV (BLNP)	−2.32	−3.23	—	−2.35	2.07	—
	Belle (New)	—	−2.29	—	—	2.54	—

Form-Factors	Fit Index	$[B^0 \to \pi^-]$ q^2 : 4 – 8 BaBar (11)	$[B^0 \to \pi^-]$ q^2 : 20 – 26.4 BaBar (11)	$[B^0 \to \pi^-]$ q^2 : 10 – 12 BaBar (12)	$[B^0 \to \pi^-]$ q^2 : 20 – 22 BaBar (12)	$[B^0 \to \pi^-]$ q^2 : 18 – 20 Belle (11)	$[B^0 \to \pi^+]$ q^2 : 0.0111637 – 2 Belle (13)	$[B^0 \to \pi^+]$ q^2 : 8 – 10 Belle (13)
BSZ	Fit 1A	2.46	−2.30	2.08	—	—	—	−2.42
	Fit 1B	2.52	−2.42	2.07	—	—	—	−2.41
	Fit 2A	—	—	—	—	−2.02	—	−2.43
	Fit 2B	—	—	—	—	−2.07	—	−2.42
	Fit 3A	2.40	−2.35	2.00	2.01	—	—	−2.44
	Fit 3B	2.45	−2.46	—	—	—	—	−2.43
BCL	Fit 1A	2.45	−2.30	2.07	—	—	—	−2.42
	Fit 1B	2.59	−2.56	2.07	—	—	—	−2.40
	Fit 2A	—	—	—	—	−2.03	—	−2.45
	Fit 2B	—	—	—	—	−2.18	2.00	−2.42
	Fit 3A	2.36	−2.36	—	2.00	—	—	−2.45
	Fit 3B	2.48	−2.61	—	—	—	—	−2.44

- **Fit 2B-I**: input used in *Fit 2B* without the data on $\mathcal{B}(B^0 \to \pi^-)^{[18,20]}$ (Belle 2011).
- **Fit 3B-I**: input used in *Fit 3B* without the data on $\mathcal{B}(B^0 \to \pi^-)^{[20,26.4]}$ (BaBar 2011).
- **Fit 3B-II**: input used in *Fit 3B* without the data on $\mathcal{B}(B^0 \to \pi^-)^{[18,20]}$ (Belle 2011) and $\mathcal{B}(B^0 \to \pi^-)^{[20,26.4]}$ (BaBar 2011).

Fit Scenario	BSZ χ^2/DOF	BSZ p-value (%)	BSZ $V_{ub} \times 10^3$ Frequentist	BSZ $V_{ub} \times 10^3$ Bayesian	BCL χ^2/DOF	BCL p-value (%)	BCL $V_{ub} \times 10^3$ Frequentist	BCL $V_{ub} \times 10^3$ Bayesian
F2B-I	55.4/69	88.14	3.90(14)	$3.89^{+0.14}_{-0.15}$	68.85/69	48.25	3.96(14)	$3.95^{+0.14}_{-0.15}$
F3B-I	78.86/75	35.8	3.83(14)	3.83(13)	93.6/75	7.19	3.89(14)	3.89(14)
F3B-II	72.96/74	51.25	3.88(14)	$3.87^{+0.14}_{-0.15}$	87.2/74	13.99	3.94(14)	$3.93^{+0.14}_{-0.15}$

Update: Including LMD, value :

$$|V_{ub}| = (3.91 \pm 0.13) \times 10^{-3}$$

Deviation < 1σ

NP: Analysis

- $B \to \pi$: **Fit 1:** LCSR+Lattice only. Result not affected by experimental data. **Fit 2:** Add Babar (2012) and Belle datasets. Babar (2011) excluded since correlations not provided. Including them worsens the fit. **Fit 3:** Synthetic data by normalizing $BR(B \to \tau\nu)$ with charged exp data + Fit 1. Two cases: (i) Excluding NP in $BR(B \to \tau\nu)$; (ii) Including NP in $BR(B \to \tau\nu)$.

- $B \to \rho$: Normalize binned $B \to \rho l\nu$ by integrated $B \to \pi l\nu$ corresponding to same experiment and charge. Use Fit-1 results as nuisance for the normalizing integrated $B \to \pi l\nu$ modes.

$$\mathcal{B}(B \to \tau\nu) = \frac{\tau_B}{8\pi} m_B m_\tau f_B^2 G_f^2 V_{ub}^2 \left(1 - \frac{m_\tau^2}{m_B^2}\right) \left|1 + C_{V_1} - C_{V_2} + \frac{m_B^2}{m_\tau (m_b + m_u)} C_P\right|^2$$

$$\mathcal{B}(\bar{B}^0 \to \pi^+ l\nu)_{\text{Belle}} = (1.49 \pm 0.09 \pm 0.07) \times 10^{-4}$$
$$\mathcal{B}(B^- \to \pi^0 l\nu)_{\text{Belle}} = (0.80 \pm 0.08 \pm 0.04) \times 10^{-4}$$
$$\mathcal{B}(\bar{B}^0 \to \pi^+ l\nu)_{\text{Babar}} = (1.41 \pm 0.05 \pm 0.07) \times 10^{-4}$$

$$R(\pi) = \frac{\Gamma(B \to \pi\tau\nu)}{\Gamma(B \to \pi\mu\nu)}, \qquad R_\mu^\tau(\pi) = \frac{\Gamma(B \to \tau\nu)}{\Gamma(B \to \pi\mu\nu)}$$
$$R_\tau^\tau(\pi) = \frac{\Gamma(B \to \tau\nu)}{\Gamma(B \to \pi\tau\nu)}, \qquad R_\tau^\mu(\pi) = \frac{\Gamma(B \to \mu\nu)}{\Gamma(B \to \pi\tau\nu)}$$
$$R(\rho) = \frac{\Gamma(B \to \rho\tau\nu)}{\Gamma(B \to \rho\mu\nu)}, \qquad R_\mu^\tau(\rho) = \frac{\Gamma(B \to \tau\nu)}{\Gamma(B \to \rho\mu\nu)}$$
$$R_\tau^\tau(\rho) = \frac{\Gamma(B \to \tau\nu)}{\Gamma(B \to \rho\tau\nu)}, \qquad R_\tau^\mu(\rho) = \frac{\Gamma(B \to \mu\nu)}{\Gamma(B \to \rho\tau\nu)}$$
$$R_\tau^\tau(\rho/\pi) = \frac{\Gamma(B \to \rho\tau\nu)}{\Gamma(B \to \pi\tau\nu)}, \qquad R_\mu^\tau(\rho/\pi) = \frac{\Gamma(B \to \rho\tau\nu)}{\Gamma(B \to \pi\mu\nu)}$$

$$R(\pi) < 1.6, \quad R_\mu^\tau(\pi) = 0.71 \pm 0.13, \quad R_\tau^\tau(\pi) > 0.5.$$

NP: Analysis (Tables)

Parameters	Fit-1	Fit-2	Fit-3 (No NP in $B \to \tau\nu$)
χ^2/dof	18.0939/34	75.0986/90	26.8725/52
p-value	0.988372	0.648645	0.998484
$\lvert V_{ub}\rvert$	—	0.003828(94)	—
a_0^+	0.236(14)	0.246(11)	0.2416(71)
a_1^+	-0.542(98)	-0.553(91)	-0.605(77)
a_2^+	0.48(34)	0.36(32)	0.18(27)
a_3^+	0.82(25)	0.73(24)	0.60(21)
a_1^0	0.477(95)	0.529(87)	0.497(74)
a_2^0	1.49(30)	1.58(28)	1.50(28)
a_3^0	1.72(30)	1.78(30)	1.71(30)
a_0^T	0.231(14)	0.239(13)	0.236(11)
a_1^T	-0.61(11)	-0.62(11)	-0.64(10)
a_2^T	0.15(44)	0.021(430)	-0.041(412)
a_3^T	0.50(40)	0.39(39)	0.34(38)
Observables	**Fit-1**	**Fit-2**	**Fit-3**
R(π)	0.691(15)	0.684(11)	0.681(13)
$R_\tau^\tau(\pi)$	0.988(65)	0.951(41)	0.942(53)
$R_\tau^\mu(\pi)$	0.00444(29)	0.00427(19)	0.00423(24)
$R_\mu^\tau(\pi)$	0.683(55)	0.650(31)	0.641(43)

Table 1. Fit results for the coefficients of the form factors a_n^i for the form factors $f^i(q^2)$ that contribute to semileptonic $B \to \pi$ transitions using a BSZ parametrization as mentioned in the text. The kinematic constraint $f^+(0) = f^0(0)$ is manifest in such a parametrization simply implying that $a_0^+ = a_0^0$ and hence a_0^0 has not been explicitly shown in the table. Note that the a_0^T's do not take part in semileptonic charged current $B \to \pi$ transitions within the SM and hence are simply constrained by the LCSR and Lattice datapoints.

Observables	Scenarios					
	C_{V_1}		C_{V_2}		C_P	
	Sol-1	Sol-2	Sol-1	Sol-2	Sol-1	Sol-2
	-0.20(13)	-1.80(13)	0.20(13)	1.80(13)	-0.055(36)	-0.481(36)
R(π)	0.44(15)	0.44(15)	1.00(22)	5.41(53)	–	–
$R_\tau^\tau(\pi)$	0.988(65)	0.988(65)	0.43(24)	0.080(20)	0.63(21)	0.63(21)
$R_\tau^\mu(\pi)$	0.0070(23)	0.0070(23)	0.00306(71)	0.000568(66)	0.00444(29)	0.00444(29)
$R_\mu^\tau(\pi)$	0.43(15)	0.43(15)	0.43(15)	0.43(15)	0.43(15)	0.43(15)

Table 3. The results of the observables defined in eq. (2.9) corresponding to the two NP solutions obtained from fitting the 'Fit-3' dataset considering NP effects in $\mathcal{B}(B \to \tau\nu)$. Sol-1 corresponds to the solution close to the SM. Sol-2 corresponds to the solution away from the SM.

Observables	Predictions (for $n = 3$)					
	C_{V_1}		C_{V_2}		C_P	
	Sol-1	Sol-2	Sol-1	Sol-2	Sol-1	Sol-2
	-0.20(13)	-1.80(13)	0.20(13)	1.80(13)	-0.055(36)	-0.481(36)
R(ρ)	0.34(11)	0.34(11)	0.429(58)	1.11(18)	0.5303(90)	0.4885(77)
$R_\tau^\tau(\rho)$	0.542(51)	0.542(51)	0.542(51)	0.169(33)	0.35(12)	0.38(13)
$R_\tau^\mu(\rho)$	0.0038(13)	0.0038(13)	0.00305(49)	0.00118(20)	0.00247(24)	0.00268(25)
$R_\tau^\tau(\rho/\pi)$	1.73(15)	1.73(15)	0.96(34)	0.454(45)	1.71(15)	1.57(14)
$R_\mu^\tau(\rho))$	0.187(63)	0.187(63)	0.187(63)	0.187(63)	0.184(65)	0.184(65)

Table 7. The results of the observables defined in eqs. (2.10) and (3.4) corresponding to the two NP solutions obtained from fitting to dataset defined in 'Fit-3' with NP in $B \to \tau\nu$.

Without Babar				With Babar			
n =3 (p-value 99.99%)		n = 2 (p-value 99.89%)		n =3 (p-value 96.00%)		n = 2 (p-value 93.35%)	
Parameters	fit values	Parameters	fit values	Parameters	fit values	Parameters	fit values
$a_0^{A_0}$	0.309(17)	$a_0^{A_0}$	0.316(16)	$a_0^{A_0}$	0.290(16)	$a_0^{A_0}$	0.295(15)
$a_1^{A_0}$	-0.86(16)	$a_1^{A_0}$	-0.95(13)	$a_1^{A_0}$	-0.83(16)	$a_1^{A_0}$	-0.951(13)
$a_2^{A_0}$	1.5(10)	$a_0^{A_1}$	0.249(13)	$a_2^{A_0}$	1.33(100)	$a_0^{A_1}$	0.231(11)
$a_0^{A_1}$	0.247(16)	$a_1^{A_1}$	0.424(50)	$a_0^{A_1}$	0.226(15)	$a_1^{A_1}$	0.434(49)
$a_1^{A_1}$	0.435(95)	a_0^V	0.319(17)	$a_1^{A_1}$	0.450(94)	a_0^V	0.298(15)
$a_2^{A_1}$	0.33(30)	a_1^V	-0.795(54)	$a_2^{A_1}$	0.30(30)	a_1^V	-0.778(53)
$a_1^{A_2}$	-0.45(11)	$a_1^{A_2}$	-0.468(51)	$a_1^{A_2}$	-0.36(10)	$a_1^{A_2}$	-0.408(47)
$a_2^{A_2}$	0.92(114)			$a_2^{A_2}$	0.45(109)		
a_0^V	0.310(20)			a_0^V	0.287(19)		
a_1^V	-0.79(13)			a_1^V	-0.78(13)		
a_2^V	1.84(90)			a_2^V	1.77(89)		

Table 5. Fit results for the coefficients of the form factors a_n^i for the vector (V), axial-vector (A's) and tensor (T's) form factors that contribute to semileptonic $B \to \rho$ transitions using a BSZ parametrization as mentioned in the text with and without the inclusion of the Babar data from ref. [25]. We use the results of the 'Fit-1' dataset (table 1) as nuisance for the integrated $B \to \pi$ decays used to normalize the binned $B \to \rho$ data. For $B \to \rho$, we use $n = 3$ and $n = 2$ parametrization while for $B \to \pi$ we use $n = 4$. Note that the $a_n^{T_{(\epsilon)}}$'s do not take part in semileptonic charged current $B \to \rho$ transitions within the SM and hence are simply constrained by the LCSR datapoints.

Observables	SM Predictions			
	Without Babar combined data		With Babar combined data	
	n=2	n=3	n=2	n=3
R(ρ)	0.5303(57)	0.5381(79)	0.5287(61)	0.5352(84)
$R_\tau^\tau(\rho)$	0.548(52)	0.542(51)	0.655(57)	0.658(58)
$R_\tau^\mu(\rho)$	0.00246(23)	0.00244(23)	0.00294(25)	0.00295(25)
$R_\tau^\tau(\rho/\pi)$	1.70(15)	1.73(15)	1.40(10)	1.41(10)
$R_\mu^\tau(\rho/\pi)$	1.163(99)	1.182(100)	0.956(70)	0.958(70)
$R_\mu^\tau(\rho)$	0.290(27)	0.292(27)	0.346(30)	0.352(31)

Table 6. SM predictions for the observables defined in (2.10), $R_\tau^\tau(\rho/\pi)$ and $R_\mu^\tau(\rho/\pi)$ the full allowed kinematic ($0 \le q^2 \le 20.29$) regions corresponding to $n = 2$ and $n = 3$ parametrizations for the BSZ form factors corresponding to the inclusion and exclusion of the Babar data from [25].

NP: Analysis (Figures)

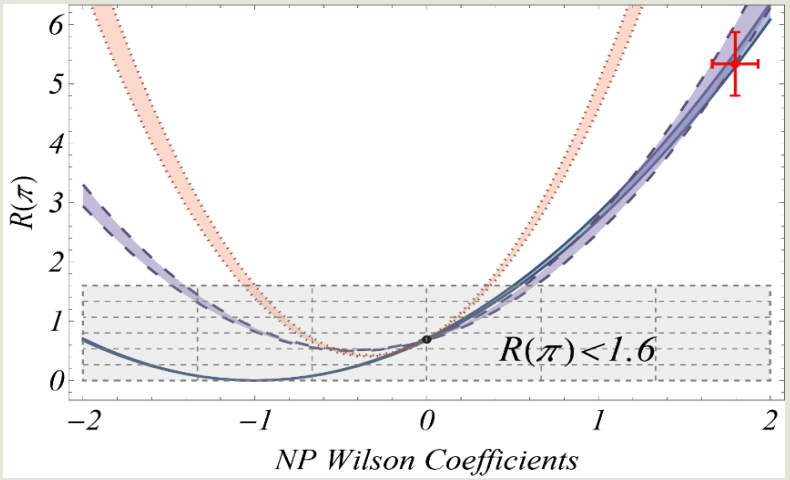

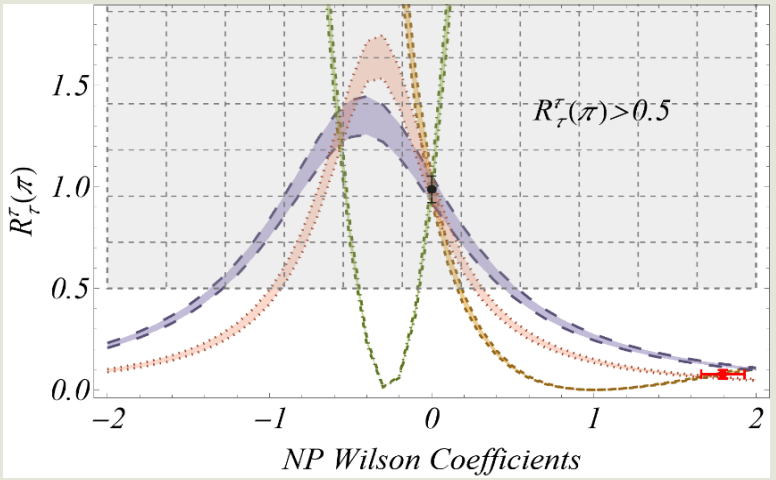

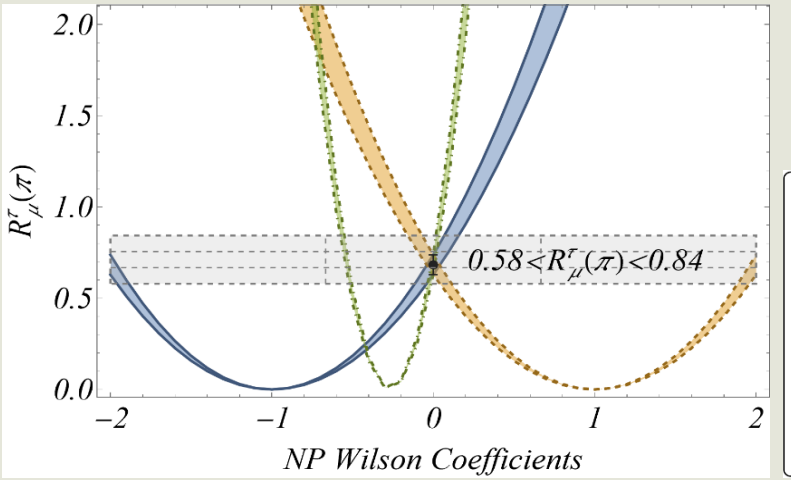

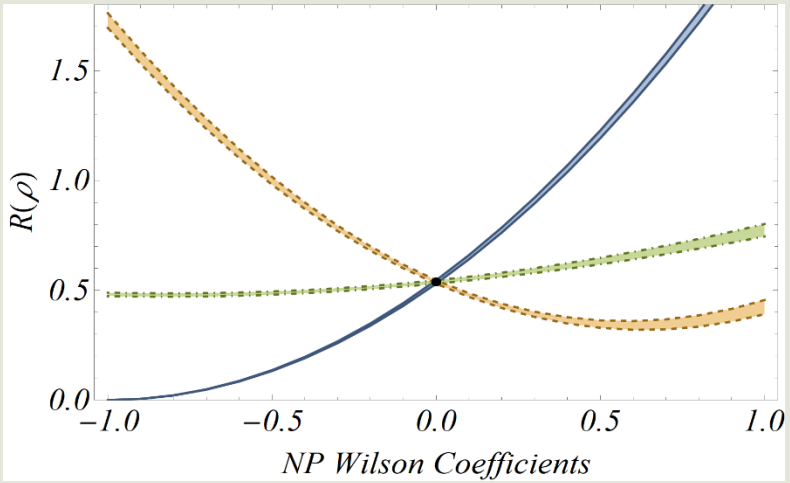

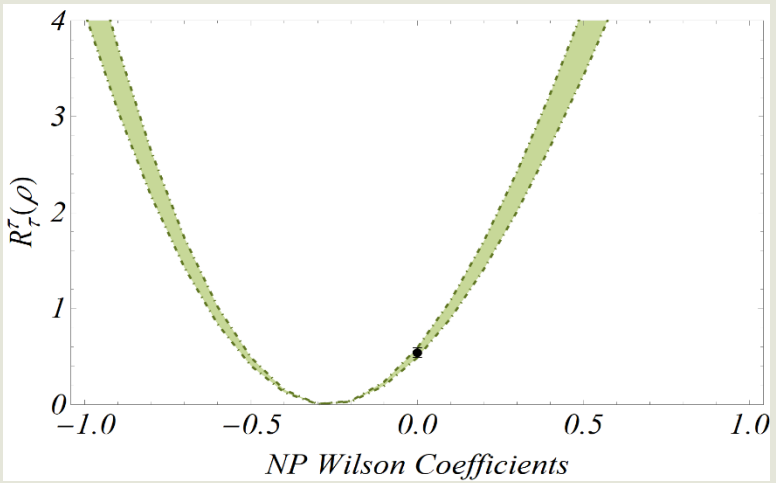

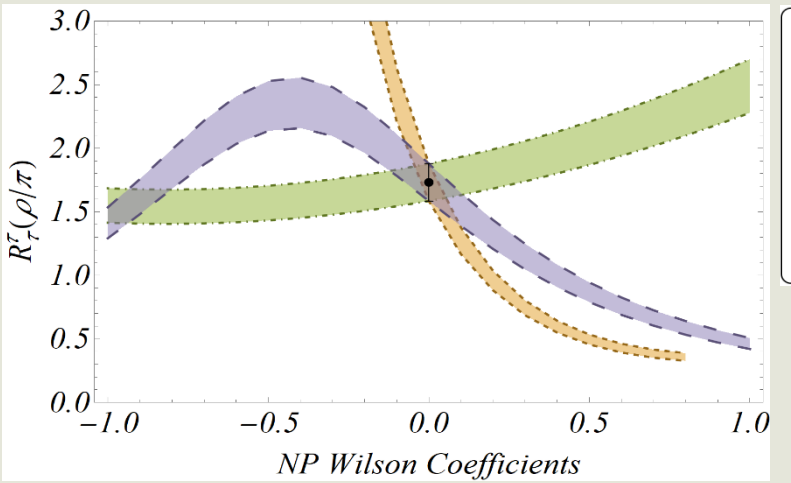

Observable predictions

- Forward-backward asymmetry is defined as

$$\mathcal{A}_{FB}^{\ell} = \frac{\int_0^1 \frac{d\Gamma}{d\cos\theta} d\cos\theta - \int_{-1}^0 \frac{d\Gamma}{d\cos\theta} d\cos\theta}{\int_{-1}^1 \frac{d\Gamma}{d\cos\theta} d\cos\theta}, \tag{3.5}$$

  where θ is the angle that ℓ (μ or τ) makes with the B in the rest frame of $\tau\bar{\nu}$.

- τ polarisation asymmetry,

$$P_\tau = \frac{\Gamma(\lambda_\tau = 1/2) - \Gamma(\lambda_\tau = -1/2)}{\Gamma(\lambda_\tau = 1/2) + \Gamma(\lambda_\tau = -1/2)} \tag{3.6}$$

  where P_τ is the τ-polarisation asymmetries in $B^0 \to \pi^+\tau\nu$ and $B^0 \to \rho^+\tau\nu$ decays.

- ρ-longitudinal polarisation ($\rho^+ \to \pi^+\pi^0$),

$$P_\rho = \frac{\Gamma(\lambda_{\rho=0})}{\Gamma(\lambda_{\rho=0}) + \Gamma(\lambda_{\rho=1}) + \Gamma(\lambda_{\rho=-1})}, \tag{3.7}$$

- The observable F_H^ℓ:[7]

$$F_H^\ell = 1 + \frac{2}{3}\frac{1}{\Gamma}\frac{d^2}{d(\cos\theta)^2}\frac{d\Gamma}{d\cos\theta}, \tag{3.8}$$

Observables	Values			
	Fit-1		Fit-2	
	$\ell = \mu$	$\ell = \tau$	$\ell = \mu$	$\ell = \tau$
$A_{\rm FB}^l$	0.00484(21)	0.2565(31)	0.00484(12)	0.2564(26)
P^l	-0.98679(59)	-0.229(21)	-0.98683(37)	-0.234(19)

Table 8. SM values for angular observables related to the semileptonic $B \to \pi$ transitions. The values are provided for both muonic and tauonic final states corresponding to the Fit-1 and Fit-2 scenarios described in the text.

Observables	Values							
	Without Babar				With Babar			
	n=2		n=3		n=2		n=3	
	$\ell = \mu$	$\ell = \tau$	$\ell = \mu$	$\ell = \tau$	$\ell = \mu$	$\ell = \tau$	$\ell = \mu$	$\ell = \tau$
$A_{\rm FB}^l$	0.532(60)	-0.197(13)	0.482(77)	-0.215(24)	0.553(64)	-0.202(15)	0.530(80)	-0.212(26)
P^l	-0.99088(47)	-0.538(13)	-0.99120(54)	-0.545(20)	-0.99055(49)	-0.524(13)	-0.99070(55)	-0.526(21)
P^ρ	0.490(16)	0.474(14)	0.473(29)	0.458(28)	0.485(18)	0.471(15)	0.478(30)	0.464(29)

Table 9. SM values for angular observables related to the semileptonic $B \to \rho$ transitions for both $n = 2$ and $n = 3$ BSZ parametrizations of the form factors. The values are provided for both muonic and tauonic final states and corresponding to both the inclusion and exclusion of the Babar data from [25].

THANK YOU!